Institutionen för systemteknik
Department of Electrical Engineering

Master's Thesis

Mean Value Model of the Gas Temperature at the Exhaust Valve

Master's thesis in Vehicular Systems
at Linköping Institute of Technology
By

Filip Ainouz and Jonas Vedholm

LiTH-ISY-EX--09/4296--SE

Linköping 2009

Linköpings universitet
TEKNISKA HÖGSKOLAN

Department of Electrical Engineering
Linköpings universitet
SE-581 83 Linköping, Sweden

Linköpings tekniska högskola
Linköpings universitet
581 83 Linköping

Mean Value Model of the Gas Temperature at the Exhaust Valve

Master's Thesis performed at:
Division of Vehicular Systems
Department of Electrical Engineering
Linköping Institute of Technology
Performed by

Filip Ainouz and Jonas Vedholm

LiTH-ISY-EX--09/4296--SE

Supervisor:	**Per Öberg** ISY, Linköpings universitet **Oskar Leufven** ISY, Linköpings universitet **Lars Eriksson** ISY, Linköpings universitet
Examinator:	**Lars Eriksson** ISY, Linköpings universitet

Linköping, 08 September, 2009

Avdelning, Institution
Division, Department

Vehicular Systems
Department of Electrical Engineering
Linköpings universitet
SE-581 83 Linköping, Sweden

Datum
Date

2009-09-008

Språk
Language

☐ Svenska/Swedish
☒ Engelska/English
☐ ______________

Rapporttyp
Report category

☐ Licentiatavhandling
☒ Examensarbete
☐ C-uppsats
☐ D-uppsats
☐ Övrig rapport
☐ ______________

ISBN
—

ISRN
LiTH-ISY-EX--09/4296--SE

Serietitel och serienummer
Title of series, numbering

ISSN
—

URL för elektronisk version

`http://www.fs.isy.liu.se`
`http://urn.kb.se/resolve?urn=urn:nbn:se:liu:diva-ZZZZ`

Titel
Title

Medelvärdesmodell av gastemperaturen vid avgasventilen
Mean Value Model of the Gas Temperature at the Exhaust Valve

Författare
Author

Filip Ainouz and Jonas Vedholm

Sammanfattning
Abstract

Over the years many investigations of the gas temperature at the exhaust valve have been made. Nevertheless the modeling of the gas temperature still remains an unsolved problem. This master thesis approaches the problem by attempting to model the exhaust gas temperature by using the standard sensors equipped in SI engines, together with an in-cylinder pressure sensor which is needed in order to develop certain models. The concept in the master thesis is based upon a parameterization of the ideal Otto cycle with tuning parameters which all have physical meanings. Input variables required for the parameterization model is obtained from a fix point iteration method. This method was developed in order to improve the estimates of residual gas fraction, residual gas temperature and variables dependent of those, such as temperature at intake valve closing. The mean value model of the temperature, at the exhaust valve, is based upon the assumption of the ideal gas law, and that the burned gases undergoe a polytropic expansion into the exhaust manifold. Input variables to the entire model are intake manifold pressure, exhaust manifold pressure, intake manifold temperature, engine speed, air mass flow, cylinder pressure, air-to-fuel equivalence ratio, volume, and ignition timing. A useful aspect with modeling the exhaust gas temperature is the possibility to implement it in turbo modeling. By modeling the exhaust gas temperature the control of the turbo can be enhanced, due to the fact that energy is temperature dependent. Another useful aspect with the project is that the model can be utilized in diagnostics, to avoid hardware redundency in the creation of the desired residuals.

Nyckelord
Keywords

Mean Value Model, Exhaust Temperature, Four Stroke Model, Fix Point Iteration, Analytic Model

Abstract

Over the years many investigations of the gas temperature at the exhaust valve have been made. Nevertheless the modeling of the gas temperature still remains an unsolved problem. This master thesis approaches the problem by attempting to model the exhaust gas temperature by using the standard sensors equipped in SI engines, together with an in-cylinder pressure sensor which is needed in order to develop certain models. The concept in the master thesis is based upon a parameterization of the ideal Otto cycle with tuning parameters which all have physical meanings. Input variables required for the parameterization model is obtained from a fix point iteration method. This method was developed in order to improve the estimates of residual gas fraction, residual gas temperature and variables dependent of those, such as temperature at intake valve closing. The mean value model of the temperature, at the exhaust valve, is based upon the assumption of the ideal gas law, and that the burned gases undergoe a polytropic expansion into the exhaust manifold. Input variables to the entire model are intake manifold pressure, exhaust manifold pressure, intake manifold temperature, engine speed, air mass flow, cylinder pressure, air-to-fuel equivalence ratio, volume, and ignition timing. A useful aspect with modeling the exhaust gas temperature is the possibility to implement it in turbo modeling. By modeling the exhaust gas temperature the control of the turbo can be enhanced, due to the fact that energy is temperature dependent. Another useful aspect with the project is that the model can be utilized in diagnostics, to avoid hardware redundency in the creation of the desired residuals.

Acknowledgments

Over the course of this master thesis several people have been involved and engaged in the project who all deserve many thanks. First of all Lars Eriksson, at Vehicular System who gave us the opportunity to conduct this master thesis. Our supervisors Per Öberg and Oskar Leufven also deserve a special thanks for interesting discussions and viewpoints throughout the thesis. We would also like to thank the division of Vehicular Systems at Linköpings Institute of Technology, for giving us the opportunity to conduct engine measurements on an experimental engine setup. We will also like to thank Tobias Lindell who helped us prepare the engine setup, and later supervised the measurements in the engine lab, and Andreas Thomasson who reviewed the thesis.

We would also like to thank the employees at Vehicular System for a warm welcome and a pleasant and helpful environment during the work with the thesis. Finally we would like to thank our beloved families and friends for their support throughout the thesis.

Filip Ainouz and Jonas Vedholm

Contents

1 Introduction **1**
- 1.1 Background . . . 1
- 1.2 Limitations . . . 2

2 Fundamental Approach **3**
- 2.1 Overall objective . . . 3
- 2.2 Model validations . . . 4
- 2.3 Measurements . . . 4

3 Phase one: Estimates of p_{IVC}, T_{IVC} and x_r at IVC **9**
- 3.1 Classification of variables and parameters in submodel one . . . 10
- 3.2 Modeling of p_{IVC} . . . 10
  - 3.2.1 Estimation of c_{pim} . . . 10
  - 3.2.2 Validation of p_{IVC} . . . 10
- 3.3 Modeling of $\dot{m}_{af}$ and m_{af} . . . 10
- 3.4 Modeling of T_{IVC}, x_r and T_r . . . 12
  - 3.4.1 Rejected methods . . . 12
  - 3.4.2 Chosen method . . . 12
  - 3.4.3 Validations of T_{IVC}, x_r and T_r . . . 14
- 3.5 Other parameters to estimate in phase one . . . 15
  - 3.5.1 Estimation of the polytropic exponent γ . . . 15
  - 3.5.2 Estimates of θ_{IVC} and θ_{EVO} . . . 15
  - 3.5.3 Estimates of $(A/F)_s$, n_r and n_{cyl} . . . 15

4 Phase two: Modeling of in Cylinder Pressure and Temperature **17**
- 4.1 Classification of variables and parameters in submodel two . . . 18
- 4.2 Modeling of cylinder pressure from IVC to EVO . . . 18
- 4.3 Model equations in phase two . . . 18
- 4.4 Parameter estimates in submodel two . . . 21
  - 4.4.1 Estimation of γ_c . . . 21
  - 4.4.2 Estimates of γ_e, η_{ht}, $\Delta\theta_d$ and $\Delta\theta_b$ . . . 21
  - 4.4.3 Estimates of q_{HV} and c_v . . . 21
- 4.5 Experimental validation of phase two . . . 22
  - 4.5.1 Validation of γ_e and γ_c . . . 22
  - 4.5.2 Validation of the whole submodel . . . 22

4.6 Analysis of cycle to cycle variations 23

5 Phase three: Modeling of Gas Temperature at the Exhaust Valve 29

5.1 Classification of variables and parameters in submodel three 29
5.2 Modeling of the mean value temperature at the exhaust valve . . . 30
  5.2.1 Blowdown phase, $\theta \in [\theta_{EVO}, \theta_{BL}]$ 30
  5.2.2 Exhaust phase, $\theta \in [\theta_{BL}, \theta_{IVO}]$ 31
  5.2.3 Mean value exhaust temperature T_{ev} 31
5.3 Experimental validation of T_{ev} 31
  5.3.1 Validation result 31
5.4 Other parameter estimates in phase three 33
  5.4.1 Estimates of c_p and R 33
  5.4.2 Estimation of h_{cv} 33
5.5 Model results 33
  5.5.1 T_{ev}'s dependency of mass flow 33
  5.5.2 Varying intake manifold pressure 33
  5.5.3 Varying engine speed 35
  5.5.4 The effect of fuel enrichment 35
  5.5.5 Altering ignition timing 37

6 Conclusion 39

6.1 T_{ev} decreases with increasing p_{im} 39
6.2 T_{ev} increases with N 39
6.3 T_{ev}'s dependency of λ 40
6.4 The ignition timings influence on T_{ev} 40
6.5 Correlation between mass flow and T_{ev} 40
6.6 Future work 40

Nomenclature 44

Bibliography 45

Chapter 1

Introduction

This Master thesis has been carried out at the division of vehicular systems at the Department of Electrical Engineering (ISY), Linköping Institute of Technology, Sweden. The goal with the Master thesis is to develop a mean value model of the gas temperature at the exhaust valve. The main purpose of the model is to integrate it in a larger research project, where the aim is to develop a model of a two stage turbo engine.

1.1 Background

There have been many investigations of the exhaust valve temperature which is interesting in several aspects of engine control. In turbocharged engines the energy from the exhaust gases is used to compress the air in the intake manifold, which increases the possible power output from the engine. In order to control the turbo speed, good estimates of the energy flow to the turbine is required. By modeling the exhaust gas temperature, the control of the turbo can be enhanced, due to the fact that exhaust energy is temperature dependent.

Another useful aspect with the project, is that further precision of the exhaust gas temperature estimates can prevent the two stage turbo, as well as the catalyst to take permanent damage, due to high temperatures. Besides the potential repair cost this is useful in an environmental aspect since damage to the catalyst decreases the conversion efficiency and thereby increases the noxious emissions.

The temperature at the exhaust valve has been investigated by many authors. In [9] a thermodynamic cycle simulation is used to model the exhaust valve temperature. This model is based upon the second law of thermodynamics. In [3] cylinder pressure data together with a two zone combustion model of the gas exchange and heat transfer, is used to calculate the temperature of the gas flowing out through the exhaust port. In [4] a method is used to measure the instantaneous exhaust gas temperature by thermocouples. Experimental studies of the periodic heat transfer coefficient in the entrance zone of an exhaust pipe is made in [8]. In [2] the exhaust valve temperature is modeled as an affine function of the mass flow: $T_{ev} = T_{cyl,0} + \dot{m}_e K_t$, where $T_{cyl,0}$ and K_t are tuning constants.

This linear model gives good agreement with measurement data, when $\lambda = 1$ and optimal ignition timing $\theta_{ign} = \theta_{ign,opt}$, but needs to be extended for usage at other engine conditions.

1.2 Limitations

Limitations during the development phase have been the project time and the number of measurements that could be obtained. In order to obtain accurate measurements the temperatures must be stabilized, which takes approximately 10-15 minutes depending on the operating point. Therefore the number of operating points has been limited. Since only one measurement series was made, all the validations in the model were made by using the same data as for the estimates. Other limitations are the accuracy of the sensors and that opening and closing timings of the intake and exhaust valves are not known exactly. The absence of a sensor, measuring the heat flux in the entrance zone of the exhaust pipe, was also an issue. The engine operating points were also limited by the temperature restrictions of the engine setup.

Chapter 2

Fundamental Approach

The goal with this thesis is to produce a mean value model of the exhaust temperature, as a function of engine operating point, air-to-fuel ratio and ignition timing. The model is divided into three subphases which are explained in section 2.1. The measurement setup and an explanation of how the measurements were performed along with limitations, are described in section 2.3.

2.1 Overall objective

In order to develop a mean value temperature model, an approach is used where the problem is divided into three subphases. Input variables to the whole model are intake manifold pressure p_{im}, exhaust manifold pressure p_{em}, intake manifold temperature T_{im}, engine speed N, air mass flow $\dot{m}_a$, cylinder pressure p_{cyl}, air-to-fuel equivalence ratio λ, volume V and ignition timing θ_{ign}. The cylinder pressure p_{cyl} is needed in order to develop and validate models but is not needed as input singnal to the created model. Output result is mean value temperature at the exhaust valve T_{ev}. The three submodels are enumerated below:

1. Develop a model of the residual gas fraction x_r, the cylinder pressure p_{IVC} and the cylinder temperature T_{IVC}, at intake valve closing (IVC). This work is made in chapter 3.

2. Implement a four stroke cylinder model of an SI engine, based upon the ideas in Eriksson and Andersson [5]. This is made in chapter 4.

3. Develop a model of the mean value gas temperature at the exhaust valve, which is made in chapter 5.

The submodels are linked together as follows: the pressure and temperature at IVC depends on the fraction and the temperature of the residual gas. The modeled p_{IVC}, T_{IVC} and x_r in submodel one, are used as input values to the four stroke model. The accuracy of those will influence the precision of the computed pressure and temperature traces in the cylinder. The pressure and temperature traces from phase two is used in phase three, to develop a mean value model of the temperature at the exhaust valve. A schematic view of the submodels and their relations can be seen in figure 2.1.

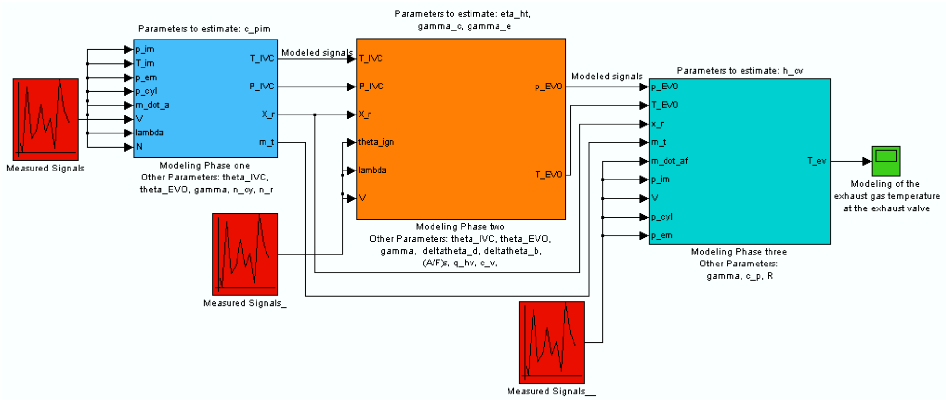
Parameters to estimate: c_pim
p_im
T_im
p_em
p_cyl
m_dot_a
V
lambda
N
T_IVC
P_IVC
X_r
m_t
Measured Signals
Modeling Phase one
Other Parameters: theta_IVC,
theta_EVO, gamma, n_cy, n_r
Modeled signals
Parameters to estimate: eta_ht,
gamma_c, gamma_e
T_IVC
P_IVC
X_r
theta_ign
lambda
V
p_EVO
T_EVO
Measured Signals_
Modeling Phase two
Other Parameters: theta_IVC, theta_EVO,
gamma, deltatheta_d, deltatheta_b,
(A/F)s, q_hv, c_v,
Modeled signals
Parameters to estimate: h_cv
p_EVO
T_EVO
x_r
m_t
m_dot_af
p_im
V
p_cyl
p_em
T_ev
Modeling Phase three
Other Parameters:
gamma, c_p, R
Modeling of the
exhaust gas temperature
at the exhaust valve
Measured Signals__

Figure 2.1. Overview of the complete model. The input signals to the whole model are p_{im}, p_{em}, T_{im}, N, $\dot{m}_a$, p_{cyl}, λ, V and θ_{ign}. Output signal is the mean value temperature at the exhaust valve T_{ev}.

2.2 Model validations

The submodels are validated directly after the modeling work in each chapter. The validations are foremost made against measured signals and secondary validated against other known relations. The entire modeling work is validated in a bottom-top order, i.e. first submodel one, then the second and finally the third. The validation data is based upon the engine measurements, which will be described in the next section.

2.3 Measurements

A series of measurements was conducted in order to obtain engine data, required to develop and verify all submodels. During pre-studies and simulations on earlier produced engine measurements, a few variables that particularly affected the pressure and temperature at the exhaust phase were identified. The main idea with the measurements was to acquire data, in order to accurately study how the engine load, engine speed, lambda and ignition timing affect the exhaust gas temperature. The measurements were conducted with an experimental engine setup operating in steady state conditions. The operating points were chosen as follows:

- Intake manifold pressure: 50, 75, 100, 125, 150 [kPa]
- Engine speed: 1500, 2000, 2500, 3000, 3500, 4000, 4500, 5000 [RPM]

- λ: 0.6, 0.7, 0.8, 0.9, 1.0, 1.1 [-]
- θ_{ign}: 14.5, 17.5, 20.5, 23.5 , 26.5, 29.5 [degree].

The engine operating points measured can be seen in figure 2.2 and 2.3. It was approximated that it takes 12-15 minutes for the different temperatures measured to stabilize, due to the mass of the engine and exhaust manifold system. During the steady state measurements approximately twenty to forty consecutive cycles were measured on all operating points, in order to obtain enough underlaying data to analyze cycle to cycle variations. Lambda and ignition timing were held at optimal conditions at the steady state measurements. Regarding the long stabilization time on temperatures, the engine speed was limited to 2500 [RPM] and the engine load to 75 [kPa] during the operating points when lambda and ignition timings were altered. This was done to obtain a well considered measurement series, regarding time and raw data. All pressures, such as the intake manifold pressure, exhaust manifold pressure and cylinder pressure for example were measured with a sampling frequency of 192 [kHz] during a one second window. The crank angle was measured at the same frequency and at every initiated engine cycle a sensor signal was measured. A motored cycle and the sensor signal was used to adjust the time offset on all measured data. Due to small fluctuations on the engine speed during the measurements, all data were interpolated and resampled to rectify the time offset errors caused by this. Temperatures were measured at the intake manifold, exhaust manifold, inside the dividing breeching at cylinder two along with the ambient temperature. The engine setup had a custom made extension that was located between the engine block and the dividing breeching which enabled easier equipping of sensors. Wall temperatures were measured at two locations at this extension together with one measurement of the engine block temperature between cylinder one and two.

The following vital signals for the project were measured: λ, N, T_{im}, p_{im}, $\dot{m}_{at}$, $t_{inj_{1-4}}$, p_{cyl}, p_e, T_{em}, T_{wall}. During the steady state measurements, where ignition timing and lambda were held optimal, a total number of 948 fired cycles were measured. During the engine points where lambda and ignition timing were altered, a total number of 276 fired cycles were measured.

Limitations during the measurements were the temperature restrictions of engine parts of the experimental engine setup, which affected the possible high load operating points with an upper limitation. Another limitation was that the temperature sensors, on the exhaust wall and in the dividing breeching, were unable to measure the gas temperature at crank angle degree, due to too long stabilization time of the sensors. Due to the absence of a sensor, it was not possible to measure the heat flux in the entrance zone of the exhaust pipe.

In the table below λ-values on the engine operating points, where fuel enrichment were used can be seen. The fuel enrichments were necessary to avoid high temperatures on engine parts on the experimental setup.

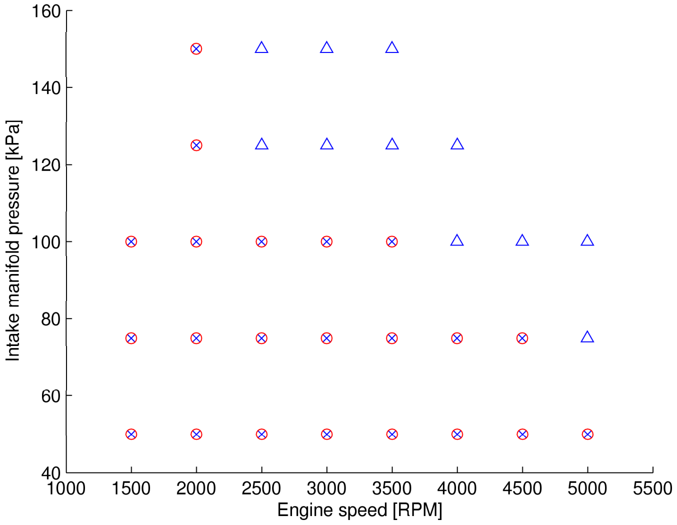

Figure 2.2. Engine operating points measured at $\theta_{ign} = \theta_{ign,opt}$ and $\lambda = 1$, except high loads where fuel enrichment were used. The engine points where fuel enrichment were used are plotted as triangles and their $\lambda - values$ can be seen in table 2.1.

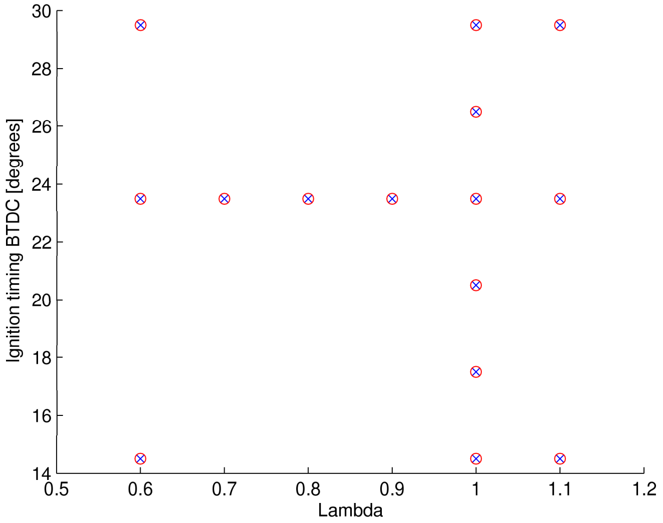

Figure 2.3. Operating points measured with altered lambda and ignition timing at engine speed 2500 [RPM] and intake manifold pressure 75 [kPa].

Operating point	$\lambda - value$
8	0.90
12	0.92
13	0.79
17	0.86
18	0.73
21	0.91
22	0.81
23	0.68
26	0.89
27	0.78
30	0.83
32	0.89
33	0.80

Table 2.1. $\lambda - values$ on the operating points where fuel enrichment were used.

Chapter 3

Phase one: Estimates of p_{IVC}, T_{IVC} and x_r at IVC

In phase one the goal is to model x_r, T_{IVC}, and p_{IVC} accurately, since these variables are inputs to phase two and have a big influence on the overall model. p_{IVC} is modeled as a constant times the intake manifold pressure. The residual gas fraction x_r, and its temperature T_r, are modeled by a fix point iteration method. Since x_r and T_r could not be measured in this thesis, the estimates could not be validated through direct comparison with experimental data. A schematic view of the submodel can be seen in figure 3.1.

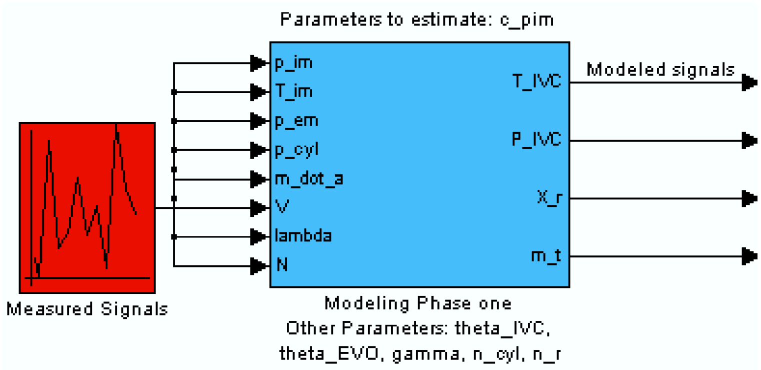
Parameters to estimate: c_pim
p_im
T_im
p_em
p_cyl
m_dot_a
V
lambda
N
T_IVC
P_IVC
X_r
m_t
Modeled signals
Measured Signals
Modeling Phase one
Other Parameters: theta_IVC,
theta_EVO, gamma, n_cyl, n_r

Figure 3.1. Overview of submodel one. A classification of the variables and parameters in the submodel is given in section 3.1.

3.1 Classification of variables and parameters in submodel one

All parameters and variables in each submodel are classified, in order to give a quick overview. They are divided into four categories; input signals, output signals, paramaters to estimate and other parameters. The parameters and variables for submodel one are defined below:

Input signals: p_{im}, T_{im}, p_{em}, p_{cyl}, $\dot{m}_a$, N, λ, V
Output signals: T_{IVC}, p_{IVC}, x_r
Parameters to estimate: c_{pim}
Other parameters: Intake valve closing θ_{IVC}, exhaust valve opening θ_{EVO}, ratio of specific heat γ, number of cylinders in engine n_{cyl}, number of revolutions per combustion cycle n_r

3.2 Modeling of p_{IVC}

The cylinder pressure at IVC is modeled as $p_{IVC} = c_{pim}p_{im}$. This method was motivated by the measured data and the models simplicity. This model gave minimum mean relative error in comparison with other models, which only had one parameter to estimate, as for example $p_{IVC} = (p_{im})^c$ or $p_{IVC} = p_{im} + c$.

3.2.1 Estimation of c_{pim}

$c_{pim} = 1.1059$ is obtained using a least square method on the measured pressure traces.

3.2.2 Validation of p_{IVC}

The modeled p_{IVC} was validated by comparing it to the measured cylinder pressure at IVC and gives a mean relative error of 3.47%. In figure 3.2 the modeled p_{IVC} is plotted against the measured cylinder pressure p_{cyl} at IVC. It can be seen that the modeled $p_{IVC} \approx p_{cyl}(\theta_{IVC})$ at most of the engine operating points.

3.3 Modeling of $\dot{m}_{af}$ and m_{af}

The total mass flow of air and fuel to the cylinders $\dot{m}_{af}$ is calculated as:

$$\dot{m}_{af} = \dot{m}_a \left(1 + \frac{1}{(A/F)_s\lambda}\right) \tag{3.1}$$

The charge mass per combustion is calculated as below, according to [6]:

$$m_{af} = \frac{\dot{m}_{af}}{n_{cyl}N/n_r} \tag{3.2}$$

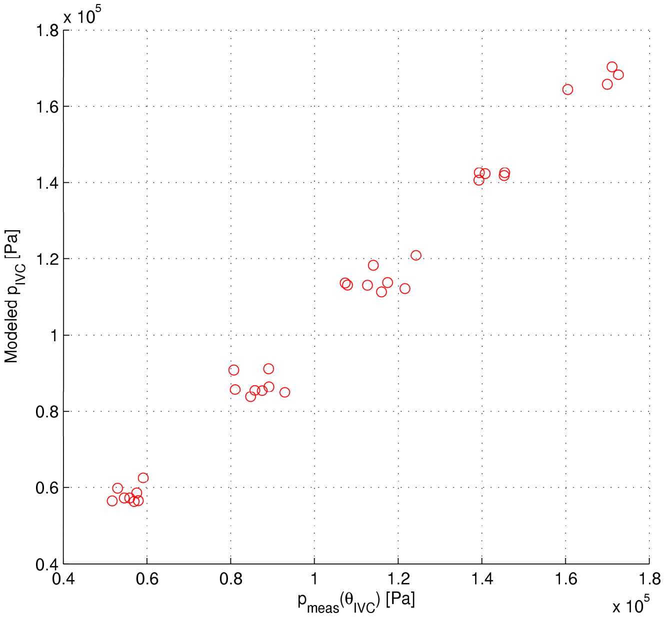

Figure 3.2. Validation of the modeled p_{IVC}. The modeled p_{IVC} is plotted against the measured pressure at IVC. It can be seen in the figure that the correlation between the modeled and measured p_{IVC} is close to linear with gradient coefficient of one. This indicates good model agreement.

n_{cyl} is the number of cylinders in the engine, and n_r is the number of revolutions per combustion cycle.

3.4 Modeling of T_{IVC}, x_r and T_r

These variables are very hard to estimate, due to that they are highly engine dependent. Since T_{IVC} and x_r have a big influence on the whole model, estimating these variables accurate were a big task in the thesis.

3.4.1 Rejected methods

Several different approaches were used to estimate T_{IVC}, x_r and T_r. The rejected methods are briefly described below:

- Fix point iteration according to [6]. This method is the easiest one to implement but is not sufficient since it disregards valve overlap. The model gives too small estimates of x_r in comparison with [7]
- Fix point iteration according to [7]. This approach is the most advanced and have several parameters that have to be determined. Due to the small numbers of measured engine operating points, these parameters were hard to estimate. The uncertainty in the parameters limited the accuracy of the model. The results obtained gave too low estimates of x_r in comparison with [7].
- Fix point iteration according to [1]. This method is close to [7] but is extended with more parameters to estimate. The model was simplified by assuming T_r and the specific heats of unburned and burned fuel, $c_{v,fc}$ and $c_{v,rg}$, to be constants. The resulting estimates of x_r were lower than the estimates in [7], although the different engine setup prevent a direct comparison.

3.4.2 Chosen method

The experience and conclusions from implementing the previous discussed methods, lead to the development of a new fix point iteration method. The approach that gave the best result was a method which was conducted over the whole combustion cycle. This model is based on nominal assumptions of the Otto cycle and therefore has as physical meaning. The method utilizes the ideal gas law $pV = mRT$ and is described below:

Equations in the iteration method

The equations are solved in the following way:

1. Assuming an initial value of x_r and T_{IVC}.

2. Calculate the total charge mass per combustion as in [6]:

$$m_t = \frac{m_{af}}{1 - x_r} \tag{3.3}$$

3. Using the ideal gas law and assuming R and m_t to be constants on the interval IVC to EVO, the mean charge temperature T can be computed using the measured pressure trace:

$$T(\theta) = \frac{T_{IVC}}{p_{IVC} V_{IVC}} p_{cyl}(\theta) V(\theta) \tag{3.4}$$

4. The temperature at EVO is calculated as:

$$T_{EVO} = \frac{T_{IVC}}{p_{IVC} V_{IVC}} p_{cyl}(\theta_{EVO}) V(\theta_{EVO}) \tag{3.5}$$

5. Assuming the blowdown phase to be polytropic with exponent γ, until the cylinder pressure has decreased down to the exhaust manifold pressure, $p_{cyl} = p_{em}$ [6]. This CAD is defined as θ_{BL}. The temperature at the blowdown phase is calculated as:

$$T(\theta) = T_{EVO} \left(\frac{p_{cyl}(\theta)}{p_{EVO}} \right)^{\frac{\gamma - 1}{\gamma}}, \theta \in [\theta_{EVO}, \theta_{BL}] \tag{3.6}$$

   The temperature inside the cylinder is decreasing down to the exhaust temperature T_e during this phase:

$$T_e = T_{EVO} \left(\frac{p_{em}}{p_{EVO}} \right)^{\frac{\gamma - 1}{\gamma}} \tag{3.7}$$

6. By assuming R to be constant during the exhaust phase and applying the ideal gas law on the modeled pressure trace, m_r can be computed:

$$m_r = m_t \frac{p_{em} V_{IVO} T_{EVO}}{p_{EVO} V_{EVO} T_e} \tag{3.8}$$

7. Assuming that the gas expands isentropically from p_{em} down to p_{im} as proposed in [6], when the intake valve opens, gives the following equation:

$$T_r = T_e \left(\frac{p_{im}}{p_{em}} \right)^{\frac{\gamma - 1}{\gamma}} \tag{3.9}$$

8. Update x_r and T_{IVC}:

$$x_r = \frac{m_r}{m_t} \tag{3.10}$$

$$T_{IVC} = x_r T_r + (1 - x_r) T_{im} \tag{3.11}$$

9. The new value of T_{IVC} is then compared to the previous. If the difference between the new value of T_{IVC} and the old value exceeds a desired limit, the iteration continues. The limit of 1 degree is chosen, since errors of this size, are considered to have small influence on the whole model agreement.

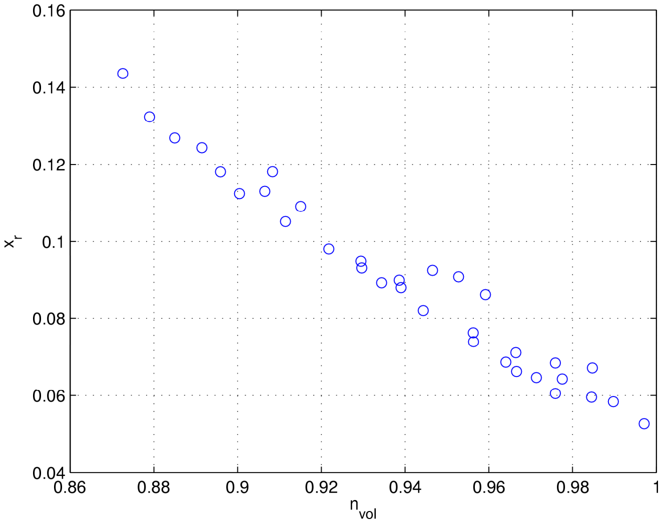

Figure 3.3. The residual gas fraction plotted against the volumetric efficiency. In the plot it can be seen that x_r shows good correlation with η_{vol}. x_r decreases when η_{vol} increases as supposed in [6], which is a sign of good modeling of x_r.

3.4.3 Validations of T_{IVC}, x_r and T_r

Since it was not possible to measure the residual gas fraction x_r, nor the residual gas temperature T_r; these two variables are hard to validate explicitly. Nevertheless the modeled x_r is only slightly smaller than in [7]. Another verification of x_r is that it shows good correlation with η_{vol}. This can be seen in figure 3.3; when η_{vol} goes towards unity x_r decreases, as in [6].

Here η_{vol} is approximated as in [6]:

$$\eta_{vol} = \frac{r_c - \left(\frac{p_{em}}{p_{im}}\right)^{\frac{1}{\gamma}}}{r_c - 1} \tag{3.12}$$

3.5 Other parameters to estimate in phase one

3.5.1 Estimation of the polytropic exponent γ

The ratio of specific heat is set to $\gamma = 1.3$ as a simplification. For an SI engine operating at stoichiometric mixture this value of γ gives good fit to pressure data according to [6].

3.5.2 Estimates of θ_{IVC} and θ_{EVO}

θ_{IVC} and θ_{EVO} are given by the engine control system. θ_{IVC} is referred to as the minimum crank angle degree (CAD), where the intake valve has completely closed. θ_{EVO} is referred to as the CAD where the exhaust valve starts to open.

3.5.3 Estimates of $(A/F)_s$, n_r and n_{cyl}

$(A/F)_s = 15.6$ $[-]$ is taken from [6]. n_r=2 and n_{cyl}=4 in the engine setup.

Chapter 4

Phase two: Modeling of in Cylinder Pressure and Temperature

Phase two extends from the closing of the intake valve IVC, until the opening of the exhaust valve EVO. The system is regarded as a closed system during this time. The concept of the model is based upon the four stroke pressure model in [5]. A schematic view of the submodel can be seen in figure 4.1.

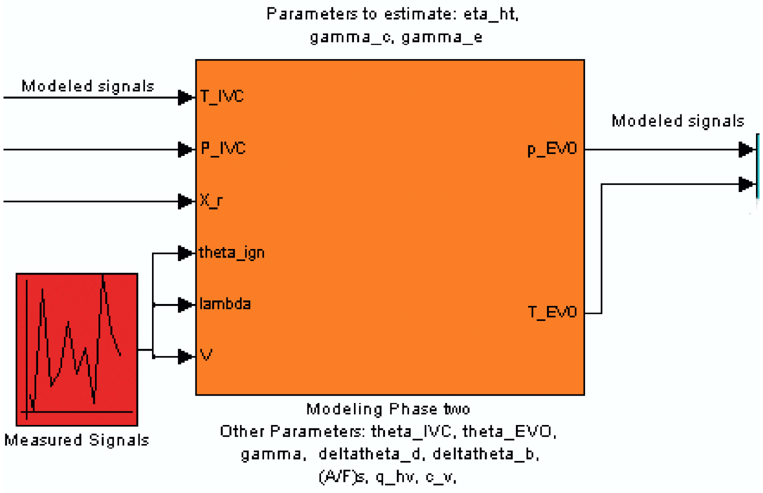
Parameters to estimate: eta_ht, gamma_c, gamma_e
Modeled signals
T_IVC
P_IVC
X_r
theta_ign
lambda
V
Measured Signals
Modeled signals
p_EVO
T_EVO
Modeling Phase two
Other Parameters: theta_IVC, theta_EVO, gamma, deltatheta_d, deltatheta_b, (A/F)s, q_hv, c_v,

Figure 4.1. Overview of submodel two. A classification of the variables and parameters in the submodel is given in section 4.1.

4.1 Classification of variables and parameters in submodel two

Input variables, parameters and output results in the submodel are defined below:

Input signals: p_{IVC}, T_{IVC}, x_r, θ_{ign}, λ
Output signals: p_{EVO}, T_{EVO}
Parameters to estimate: Heat transfer coefficient η_{ht}, ratios of specific heat at compression and expansion phases γ_c and γ_e
Other parameters: Burn angles $\Delta\theta_d$, $\Delta\theta_b$, stoichiometric air to fuel ratio $(A/F)_s$, heating value of the fuel q_{HV}, heat transfer coefficient c_v, crank angle at intake valve closing θ_{IVC}, crank angle at exhaust valve opening θ_{EVO}

4.2 Modeling of cylinder pressure from IVC to EVO

The main idea when modeling this phase, is to utilize the ideal Otto cycle and parameterize it in order to obtain an analytical model, where the parameters have physical meanings and can be tuned.

The compression phase and the expansion phase of a fired cycle are modeled as polytropic processes, which are considered to encapsulate the heat transfer. Therefore the heat transfer is not included explicitly during phase two. Based upon the ideal Otto cycle and the parameters in the submodel, a compression- and an expansion asymptote are created. The pressure trace for the combustion part is then calculated with a Viebe function, which uses interpolation between the two pressure asymptotes. The approach is based upon [5]. A schematic view of the approach is shown in figure 4.2. By assuming that the total mass m_t and the mass specific gas constant R are constants when $\theta \in (IVC, EVO)$, the ideal gas law can be used to calculate the temperature at EVO.

4.3 Model equations in phase two

The equations needed in phase two are taken from [5] and are listed below:

$$p_c(\theta) = p_{IVC}\left(\frac{V_{IVC}}{V(\theta)}\right)^{\gamma_c} \tag{4.1}$$

$$V_{IVC} = V(\theta_{IVC}) \tag{4.2}$$

$$T_c(\theta) = T_{IVC}\left(\frac{V_{IVC}}{V(\theta)}\right)^{\gamma_c - 1} \tag{4.3}$$

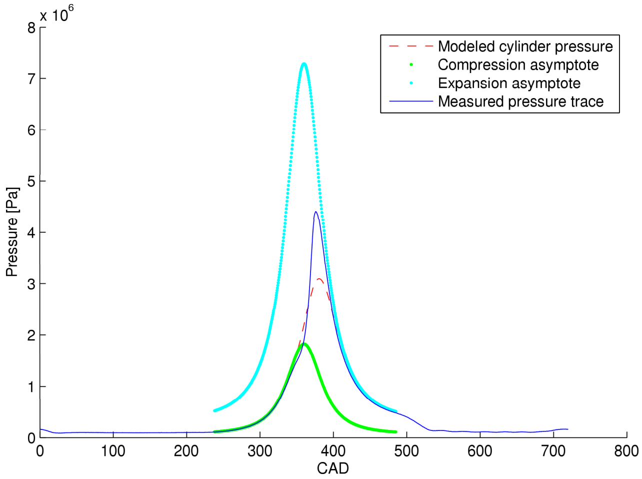

Figure 4.2. The measured mean pressure trace in the cylinder compared to the modeled pressure trace, at engine speed 2000 [rpm] and intake manifold pressure 75 [kPa]. It can be seen that the modeled pressure trace shows good agreement with the measured pressure trace, except around ppl. Since it is most important that the model agreement is good around IVC and EVO, the error in peak pressure is of less importance. The modeled compression and expansion asymptotes can also be seen in the figure. The potential offset error mentioned in 4.5.1, may have negative influence on the model agreement.

$$p_2 = p_c(\theta_c) \tag{4.4}$$

$$T_2 = T_c(\theta_c) \tag{4.5}$$

$$\theta_c = mfb_{50} - MFB_{50,OPT} \tag{4.6}$$

$$mfb_{50} = \Delta\theta_d + \frac{1}{2}\Delta\theta_b + \theta_{ign} \tag{4.7}$$

$$MFB_{50,OPT} = 8^o \tag{4.8}$$

$$p_3 = p_2 \frac{T_3}{T_2} \tag{4.9}$$

$$T_3 = T_2 + \Delta T_{comb} \tag{4.10}$$

$$\Delta T_{comb} = \eta_{ht} \frac{(1 - x_r) q_{hv} \eta_f(\lambda)}{(\lambda (A/F)_s + 1) c_v} \tag{4.11}$$

$$\eta_f(\lambda) = 0.95 \min(1; 1.2\lambda - 0.2) \tag{4.12}$$

$$p_e(\theta) = p_3 \left(\frac{V(\theta_c)}{V(\theta)} \right)^{\gamma_e} \tag{4.13}$$

$$p(\theta) = \begin{cases} p_c(\theta) & \theta_{IVC} \leq \theta \leq \theta_{soc} \\ (1 - PR(\theta)) p_c(\theta) + PR(\theta) p_e(\theta) & \theta_{soc} \leq \theta \leq \theta_{EVO} \end{cases} \tag{4.14}$$

$$PR(\theta) = 1 - e^{-a \left(\frac{\theta - \theta_{soc}}{\Delta\theta} \right)^{m+1}} \tag{4.15}$$

$$\theta_{soc} = \theta_{ign} \tag{4.16}$$

$$\Delta\theta = 2\Delta\theta_d + \Delta\theta_b \tag{4.17}$$

$$m = \frac{\ln\left(\frac{\ln(1-0.1)}{\ln(1-0.85)} \right)}{\ln(\Delta\theta_d) - \ln(\Delta\theta_d + \Delta\theta_b)} \tag{4.18}$$

$$a = -\ln(1 - 0.1) \left(\frac{\Delta\theta}{\Delta\theta_d} \right)^{m+1} \tag{4.19}$$

$$p_{EVO} = p(\theta_{EVO}) \tag{4.20}$$

$$T_{EVO} = \frac{T_{IVC}}{p_{IVC} V_{IVC}} p_{EVO} V(\theta_{EVO}) \tag{4.21}$$

4.4 Parameter estimates in submodel two

Estimates of the parameters in submodel two were made in several ways. Both through linear least-square method and by using a nonlinear least-square program called LSoptim. Because the parameters are dependent of each other they were optimized together and not individually. All parameters were optimized at the operating points where $\theta_{ign} = \theta_{ign,opt}$ and $\lambda = 1$, except the cases where fuel enrichment were used to cool down the exhaust gas temperature. This was made in order to distinguish the losses due to heat transfer, from losses due to incomplete combustion and non-optimal ignition timing.

4.4.1 Estimation of γ_c

γ_c was estimated over the compression phase, $\theta \in [\theta_{IVC}, \theta_{ign}]$, and $\gamma_c = 1.34$ was obtained by both mean least-square and LSoptim over this interval. γ_c varies much between operating points and cycle to cycle. Therefore errors in the submodel due to the estimation of γ_c are hard to prevent. The validations of γ_c are made in sections 4.5.1 and 4.5.2.

4.4.2 Estimates of γ_e, η_{ht}, $\Delta\theta_d$ and $\Delta\theta_b$

Estimation using both mean least-square method and LSoptim

The first approach was to estimate γ_e through a mean least-square method and then estimate η_{ht}, $\Delta\theta_d$ and $\Delta\theta_b$ with LSoptim. γ_e=1.23 and n_{ht}= 0.77 were found by this method. $\Delta\theta_d$ and $\Delta\theta_b$ were determined for all operating points. During the estimates, some computed values of γ_e were neglected, since they were physical too big or too small. This method gives an overall mean relative error from IVC to EVO of 6.76%, and a mean relative error at the expansion phase of 4.88%. The maximum mean relative error occurs at peak pressure location (ppl) and is 20.41%. At EVO the mean relative error is 4.80%.

Estimation using only LSoptim

The second approach was to estimate all of the parameters γ_e, n_{ht}, $\Delta\theta_d$ and $\Delta\theta_b$ with LSoptim. The estimates were $\gamma_e = 1.27$ and $n_{ht} = 0.82$. $\Delta\theta_d$ and $\Delta\theta_b$ were determined for all operating points. This method gives an overall mean relative error from IVC to EVO of 6.66%, and the mean relative error at the expansion phase is 4.74%. The maximum mean relative error occurs around the top pressure and is 22.10%. At EVO the mean relative error is 4.51%. Since these estimates give a sligthly smaller overall mean relative error than the least square method, these parameter estimates were used in the model.

4.4.3 Estimates of q_{HV} and c_v

$q_{HV} = 44.6$ $[MJ/kg]$ and $c_v = 946$ $[J/kgK]$ are taken from [6].

4.5 Experimental validation of phase two

The developed model are validated against the measured pressure data. Since the models are based upon the same data as the validation, this is not an optimal verification.

4.5.1 Validation of γ_e and γ_c

The verifications of γ_e and γ_c were made by plotting the measured and modeled pressure traces against the volume, in log-log scale, which can be seen in figure 4.3. The good match between the modeled and measured pressure traces on the straight slopes shows good modeling of γ_c and γ_e. Another verification of γ_e and γ_c is made when validating the whole submodel. The measured curve is not a perfect straight line during the compression and expansion phase, which indicates errors in the measurement data. A possible explanation to this is that the cylinder pressure sensor has an unknown offset not accounted for.

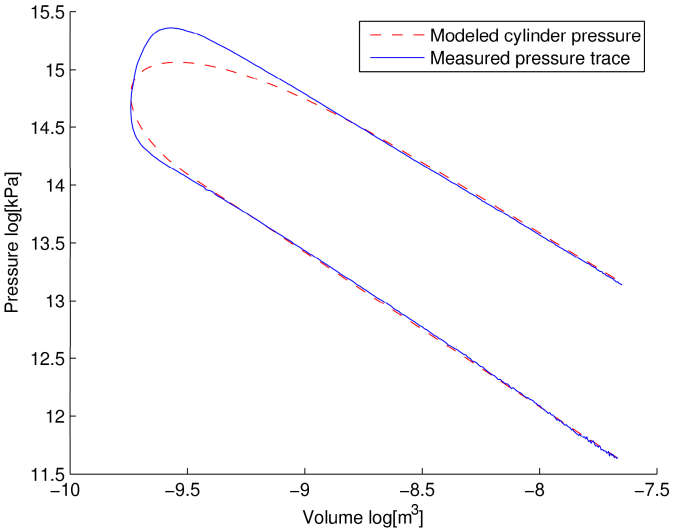

Figure 4.3. Modeled and measured pressure traces plotted against volume, in log-log scale. The match between the modeled and measured cylinder pressures on the straight slopes indicates good modeling of γ_c and γ_e. The measured curve is not a perfect straight line during the compression and expansion phase, which indicates errors in the measurement data. A possible explanation to this is that the cylinder pressure sensor has an unknown offset not accounted for.

4.5.2 Validation of the whole submodel

The four stroke model was verified by comparing the modeled pressure trace with the measured pressure trace, on the interval $\theta \in [IVC, EVO]$. The mean relative error is shown in figure 4.4. The highest deviation occurs around ppl, where the mean relative error is up to 22.10%. At the compression phase the mean relative error is 3.03% and at the expansion phase the mean relative error is 4.74%. The overall mean relative error from IVC to EVO is 6.66%, i.e. the model gives good overall fit to the measured data, except for the modeling of the peak pressure. The differences in ppl between the measured and modeled pressure traces, for all engine operating points where load and engine speed are altered, can be seen in figure 4.5. The small differences in ppl indicates that $\Delta\theta_d$ and $\Delta\theta_b$ are well estimated.

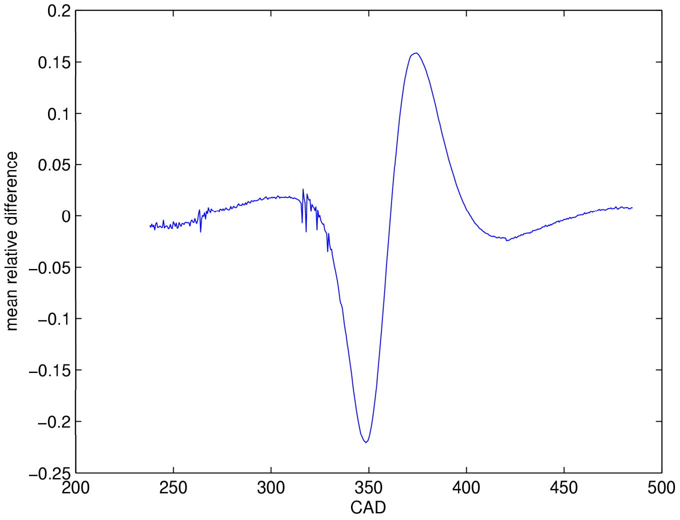

Figure 4.4. The mean relative error between the measured and modeled pressure traces in the cylinder on the interval $\theta \in [IVC, EVO]$. It can be seen that the modeled pressure is close to the measured pressure, except around ppl. The most important intervals to have good model agreement are around IVC and EVO. In the plot it can be seen that the mean relative error is close to zero at both IVC and EVO.

4.6 Analysis of cycle to cycle variations

The cycle to cycle variations between consecutive cycles are considered as an overall model limitation. Therefore they are investigated in order to obtain a lower limit of an achievable model correspondence. Differences between cycles are due to variations of the gas motion, its mixture of air, fuel and residual gases and spatial variations regarding concentration in the cylinder. Approximately twenty to forty consecutive cycles were measured on every engine operating point which allowed calculations of mean, median, min and max pressure traces. The deviations from the median cycle were calculated as a reference for an achievable model agreement. The differences in peak pressure location, PPL, were also calculated between the

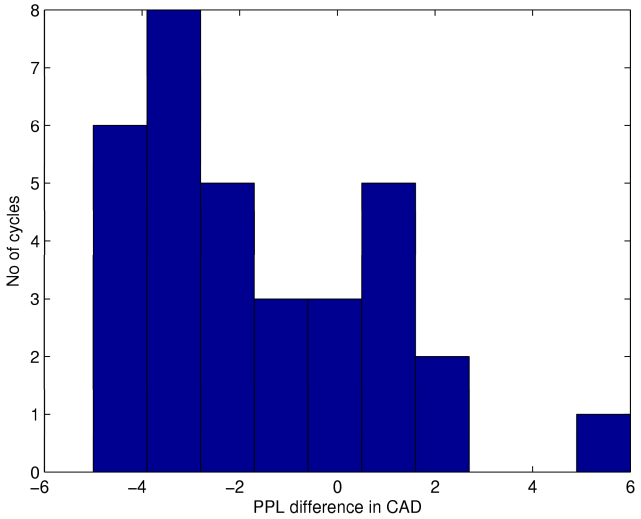

Figure 4.5. Histogram showing the differences in ppl between the modeled and measured pressure traces. The difficulties in determining the burn angles contribute the most to the differences in ppl. The variations seen in ppl emphasize the problem with parameter estimates that fit the modeled pressure to the measured on the whole interval IVC to EVO.

consecutive cycles and plotted in a histogram which can be seen in figure 4.6.

The mean, max and min pressure traces from the cylinder measurements can be seen in figure 4.7, together with corresponding data for the intake manifold traces at IVC and the exhaust manifold traces at EVO.

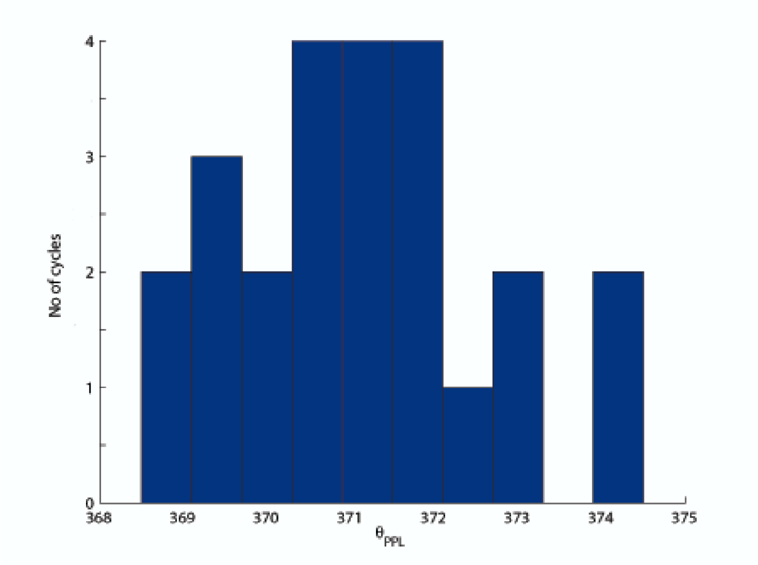

Figure 4.6. Histogram showing the differences in PPL between consecutive cycles at N 1500 [RPM] and p_{im} 75 [kPa]. It can be seen that ppl varies over a span of six degrees at this operating point. This is due to the effects mentioned in 4.6.

In figure 4.6 the pressure variations between consecutive cycles are seen and the difference in peak pressure is as high as 13.8 %. Despite the variations in the peak pressure the overall difference on the interval $\theta \in [IVC, EVO]$ is below 1%. This supports the modeling approach used in phase two.

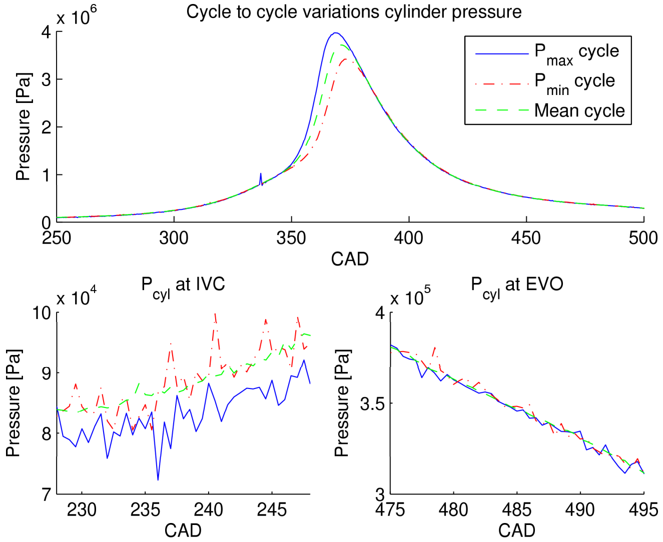

Figure 4.7. Cycle to cycle differences at N 1500 [RPM] and p_{im} 75 [kPa]. The blue solid line represents the cycle with highest peak pressure, the red dash-dotted line is the cycle with lowest peak pressure and the green dashed line is the mean-average cycle. It can be seen that the variations around IVC and EVO are small, in comparison with the differences in peak pressure.

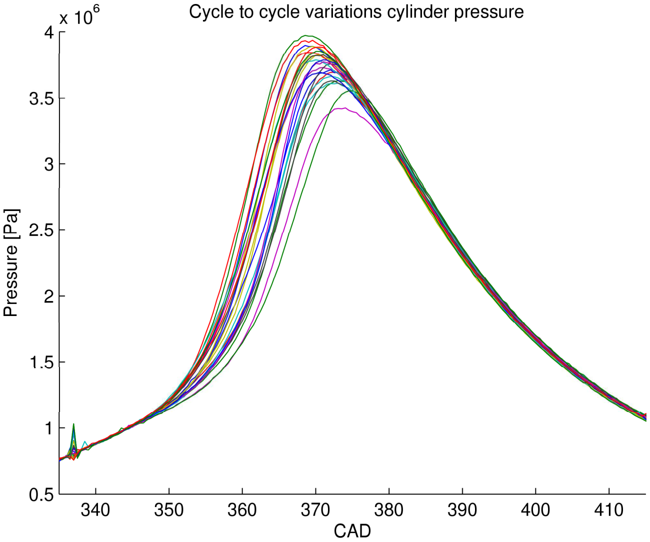

Figure 4.8. Cycle to cycle differences for all measured cycles at N 1500 [RPM] and p_{im} 75 [kPa]. Variations of the gas motion, its mixture of air, fuel and residual gases and spatial variations regarding concentration in the cylinder, explains the variations during the combustion phase and differences in peak pressure between the consecutive cycles.

Chapter 5

Phase three: Modeling of Gas Temperature at the Exhaust Valve

The aim of the Master thesis is to model the mean value temperature at the cylinder exhaust valve. The modeling of this phase was hard due to several factors such as:

- It was not possible to measure the temperature at the exhaust valve, and therefore also impossible to verify the temperature modeling directly.
- The heat transfer at the valve is very hard to estimate due to the highly varying mass flow and the high temperature of the exhaust gas. Therefore the heat losses from the exhaust valve down to the sensors are very hard to estimate.

A schematic view of the submodel can be seen in figure 5.1.

5.1 Classification of variables and parameters in submodel three

Input variables, parameters and output signals in the submodel are defined below:

Input signals: T_{EVO}, p_{EVO}, p_{cyl}, x_r, m_t, $\dot{m}_{af}$, p_{im}, p_{em}, V
Output signals: T_{ev}
Model parameters: heat transfer coefficient h_{cv}
Other parameters: standard polytropic coefficient γ, specific heat c_p, specific gas constant R

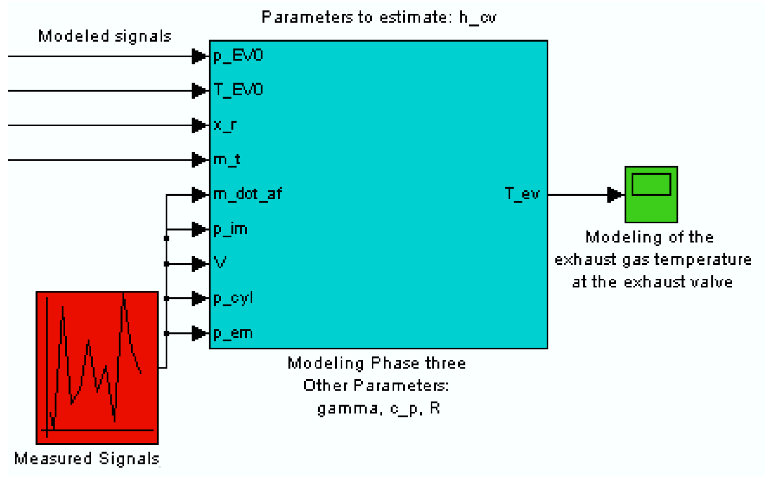
Parameters to estimate: h_cv
Modeled signals
p_EVO
T_EVO
x_r
m_t
m_dot_af
p_im
V
p_cyl
p_em
T_ev
Modeling of the exhaust gas temperature at the exhaust valve
Modeling Phase three
Other Parameters: gamma, c_p, R
Measured Signals

Figure 5.1. Overview of submodel three. A classification of the variables and parameters in the submodel is given in section 5.1.

5.2 Modeling of the mean value temperature at the exhaust valve

When the exhaust valve opens, the pressure difference between the cylinder and the exhaust manifold creates a non steady turbulent flow into the exhaust manifold. This is referred to as the blowdown phase, and continues until the cylinder pressure has decreased down to the exhaust manifold pressure [6]. During the blowdown phase the gas is assumed to undergo a polytropic expansion. The remaining gas is assumed to flow out at constant pressure and temperature [6], which is referred to as the exhaust phase. By combining the known pressure and volume traces with the ideal gas law, and assuming R to be constant, the mass flow at each crank angle can be calculated.

5.2.1 Blowdown phase, $\theta \in [\theta_{EVO}, \theta_{BL}]$

During the blowdown phase the gas is assumed to undergo an isentropic expansion process modeled as below:

$$T(\theta) = T_{EVO} \left(\frac{p_{cyl}(\theta)}{p_{EVO}} \right)^{1-1/\gamma} \tag{5.1}$$

$$m(\theta) = \frac{p_{cyl}(\theta) V(\theta)}{R T(\theta)} \tag{5.2}$$

Mass flow per crank angle:

$$\widehat{m}_e(\theta_i) = \frac{m(\theta_{i-1}) - m(\theta_i)}{\theta_i - \theta_{i-1}} \tag{5.3}$$

The remaining mass inside the cylinder after the blowdown phase m_{abl} is therefore estimated as:

$$m_{abl} = m(\theta_{BL}) \tag{5.4}$$

The temperature after the blowdown phase is:

$$T_e = T(\theta_{BL}) \tag{5.5}$$

5.2.2 Exhaust phase, $\theta \in [\theta_{BL}, \theta_{IVO}]$

The remaining gas inside the cylinder, minus the amount of residual gases, is assumed to flow out with constant temperature and pressure, T_e and P_{em}.

5.2.3 Mean value exhaust temperature T_{ev}

By making the assumptions above, of how the gas is pushed out into the exhaust system, T_{ev} can be computed as below.

$$T_{ev} = \frac{\int_{\theta_{EVO}}^{\theta_{BL}} \widehat{m}_e(\theta) T(\theta) d\theta + (m_{abl} - m_r) T_e}{m_t - m_r} \tag{5.6}$$

5.3 Experimental validation of T_{ev}

The absence of a sensor measuring the temperature at the cylinder exhaust valve, rules out the possibility of a direct validation of the submodel. Due to this, the modeled exhaust temperature at the valve is validated by using a mean value model, for the temperature drop in the dividing breeching, along with measurements of the gas temperature in the breeching. The model of the temperature drop in the pipe is taken from [2]:

$$T_{em} = T_w + (T_{ev} - T_w) e^{\frac{-h_{cv} A_i}{\dot{m}_e c_p}} \tag{5.7}$$

T_w is the mean inner wall temperature of the exhaust manifold, A_i is the inner pipe area of the exhaust pipe, between the exhaust valve and the sensor. h_{cv} is the heat transfer coefficient in the pipe, and $\dot{m}_e$ is the mean value air-fuel mass flow from one cylinder:

$$\dot{m}_e = \frac{\dot{m}_{af}}{n_{cyl}} \tag{5.8}$$

5.3.1 Validation result

In figure 5.2 T_{ev} is plotted together with T_{em} and $T_{em,meas}$. The mean relative error between T_{em} and $T_{em,meas}$ is 2.92%. This shows that the model for T_{ev} gives a good agreement with the measurements, since T_{ev} is an input variable to T_{em} in equation 5.7.

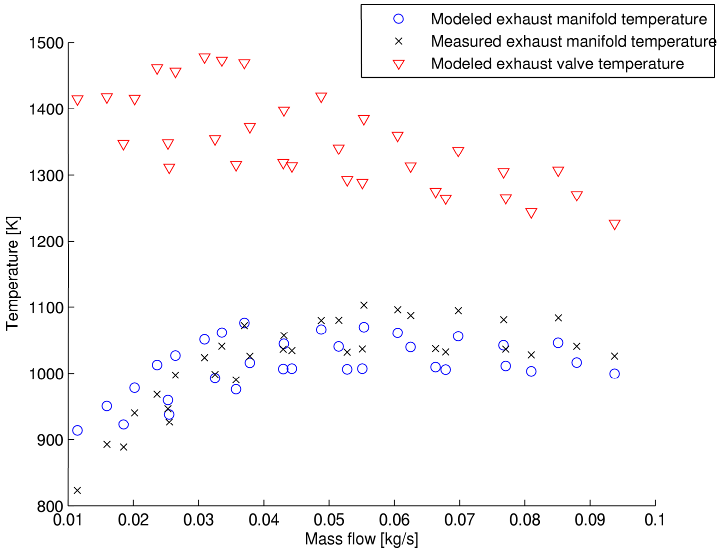

Figure 5.2. T_{ev} together with T_{em} and measured temperature in the exhaust manifold $T_{em,meas}$, plotted against $\dot{m}_{af}$. It can be seen that T_{ev} decreases slightly with increasing $\dot{m}_{af}$, which is due to fuel enrichment at higher engine loads. It can also be seen that $T_{em} \approx T_{em,meas}$. This is a sign of good modeling of T_{ev}, since T_{ev} is an input variable to T_{em} in equation 5.7. The engine operating points where fuel enrichment is made can be seen in figure 2.2 together with table 2.1.

5.4 Other parameter estimates in phase three

To estimate the cooling of the gas, from the exhaust valve to the sensor, the heat transfer coefficient h_{cv} has to be estimated. Other parameters to estimate were the specific heat at constant pressure, c_p, and the mass specific gas constant, R.

5.4.1 Estimates of c_p and R

c_p is found from the thermodynamic law $c_p = c_v \gamma$. R is taken from [6].

5.4.2 Estimation of h_{cv}

The heat transfer coefficient h_{cv} is problematic to estimate due to its dependence of mass flow. Since the flow is unsteady during the blowdown phase, it affects the boundary layer in the breeching with higher heat transfer rates as a result. Since the radiation is included, h_{cv} also depends on the temperature. In this approach h_{cv} has been modeled as a linear function of the mass flow, to keep the model simple:

$$h_{cv} = c_{hcv} \dot{m}_e \tag{5.9}$$

$c_{hcv} = 2.81 \cdot 10^5 \; [\frac{J}{m^2 kg K}]$ is obtained using LSoptim assuming T_{ev}, T_{em}, T_w and $\dot{m}_e$ are all measured and modeled correct. A big issue with this is that it is a catch 22: To model the heat transfer coefficient, the exhaust valve temperature has to be known; and to verify the exhaust valve temperature, the heat transfer has to be known. The mean value heat transfer coefficient $\overline{h}_{cv} = 3.40 \cdot 10^3 \; [\frac{W}{m^2 K}]$ estimated by LSoptim is higher than in recent reports [6], which had a cycle average heat transfer coefficient around 400 $[\frac{W}{m^2 K}]$.

5.5 Model results

The modeling work in the Master thesis indicates that the mean temperature at the exhaust valve is not strongly dependent on the engine operating point. A contradiction to [2], is that T_{ev} is not dependent of $\dot{m}_{af}$. The model results obtained in the thesis are presented below.

5.5.1 T_{ev}'s dependency of mass flow

No correlation between $\dot{m}_{af}$ and T_{ev} is found, this can be seen in figure 5.3. This is a contradiction to [2], which says that T_{ev} is increasing with $\dot{m}_{af}$.

5.5.2 Varying intake manifold pressure

It can be seen in plot 5.4 that T_{ev} decreases when p_{im} increases. A reasonable explanation is that p_{evo} is higher at higher p_{im}, which increases the blowdown phase. This leads to cooler gas temperature, see equation 5.1.

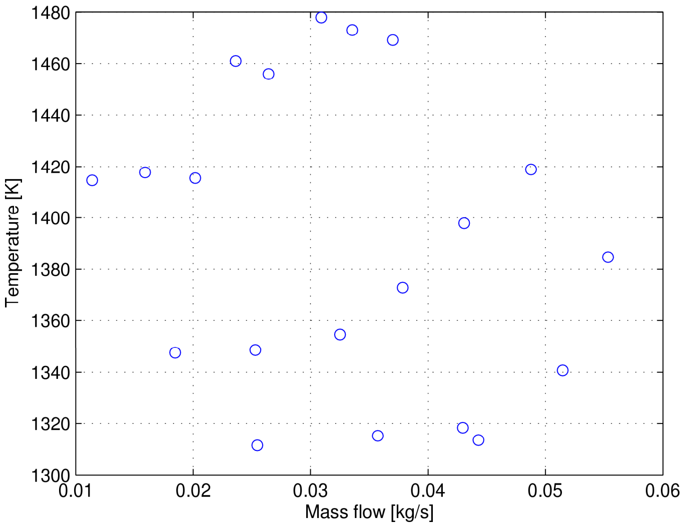

Figure 5.3. T_{ev} is plotted against $\dot{m}_{af}$ at constant $\lambda = 1$ and optimal ignition timing. These operating points can be seen in 2.2. No correlation between $\dot{m}_{af}$ and T_{ev} can be seen. This is a contradiction to [2], which stated that T_{ev} increases with increasing $\dot{m}_{af}$.

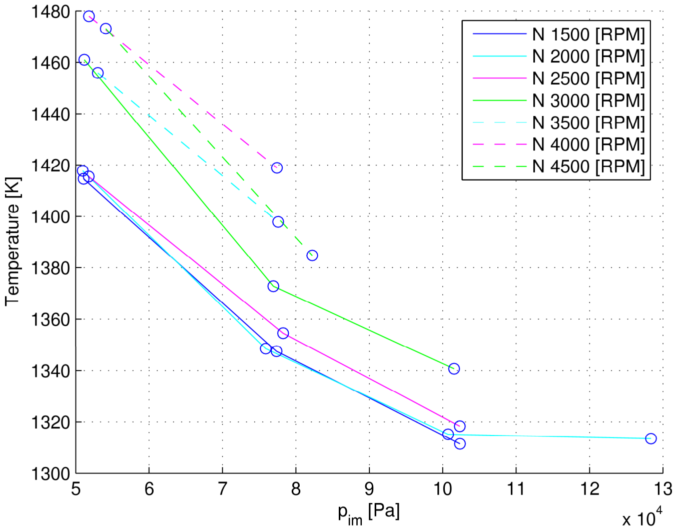

Figure 5.4. T_{ev} plotted against p_{im}, at different N and constant $\lambda = 1$. T_{ev} is seen to decrease with increasing p_{im}. A reasonable explanation may be that on high loads the difference between p_{EVO} and p_{em} is higher, which leads to a bigger expansion during the blowdown phase and a cooler gas temperature.

5.5.3 Varying engine speed

In plot 5.5 it is seen that T_{ev} increases with increasing N. A reason may be the shorter opening time of the intake and exhaust valves, which means that the gas cools down less around the valves.

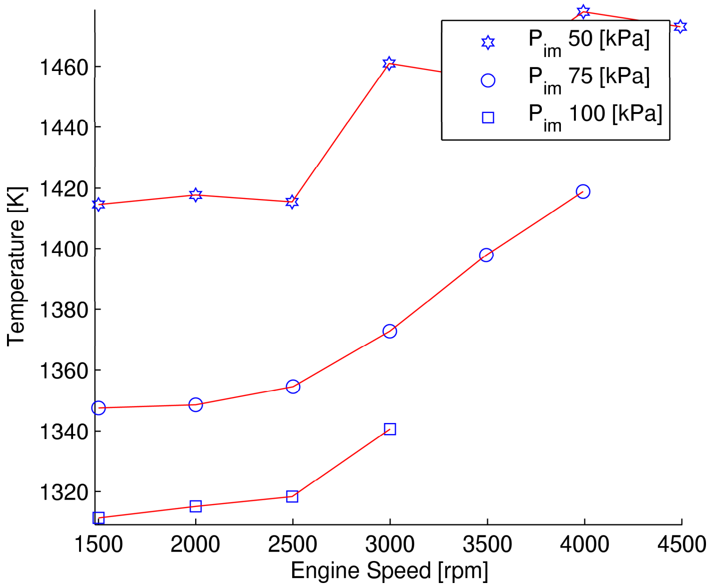

Figure 5.5. T_{ev} plotted against N, at different p_{im} and constant $\lambda = 1$. It is seen that T_{ev} increases with increasing N. A reason to this may be that the opening time of the intake and exhaust valves are shorter at higher N. This means that the gas cools down less around the valves. Higher loads are not included in the plot, since λ is not constant at these engine operating points, which prohibits any conclusion.

5.5.4 The effect of fuel enrichment

In figure 5.6 it can be seen that T_{ev} is decreasing when the air-fuel mixture is made richer than stoichiometric. Fuel enrichment effects the temperature in the cylinder in several ways. First by lowering the temperature at IVC due to the larger amount of fuel that is evaporating. Further on, the fuel enrichment also leads to incomplete combustion due to the lack of air for complete oxidation, which reduces the outgoing temperature after the combustion and expansion phase. It can also be seen that the temperature is decreasing when the mixture gets too lean. This is because the engine is more effective at leaner mixture. This means that a larger part of the fuels energy goes to work production.

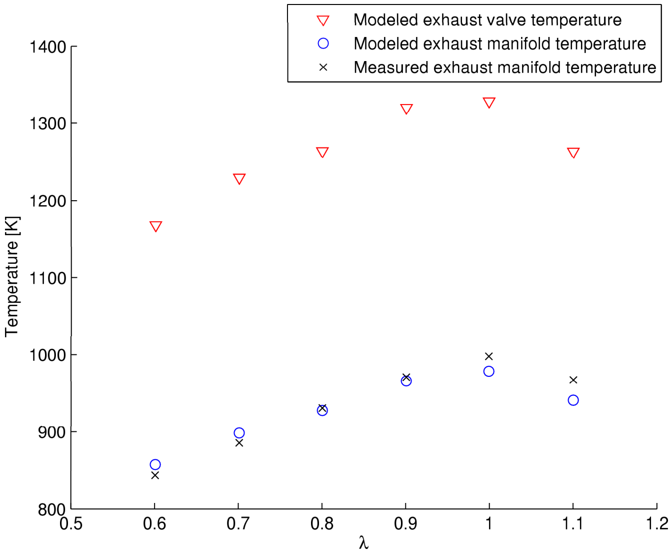

Figure 5.6. Modeled and measured temperatures when λ is altered. It can be seen that T_{ev} is decreasing when the air-fuel mixture is made richer than stoichiometric, which is explained in 5.5.4. It can also be seen that the temperature is decreasing when the mixture gets too lean. This is because the engine is more effective at leaner mixture. This means that a larger part of the fuels energy goes to work production.

5.5.5 Altering ignition timing

In figure 5.7 θ_{ign} is altered. There are signs that T_{ev} increases when θ_{ign} is moved from $\theta_{ign,opt}$. If that is the case, it is due to the reduced engine efficiency which leads to a higher exhaust temperature. It seems that the model has problems to capture variations in θ_{ign}, this may be due to the fact that γ_c and γ_e are estimated from the measurement points when $\theta_{ign} = \theta_{ign,opt}$.

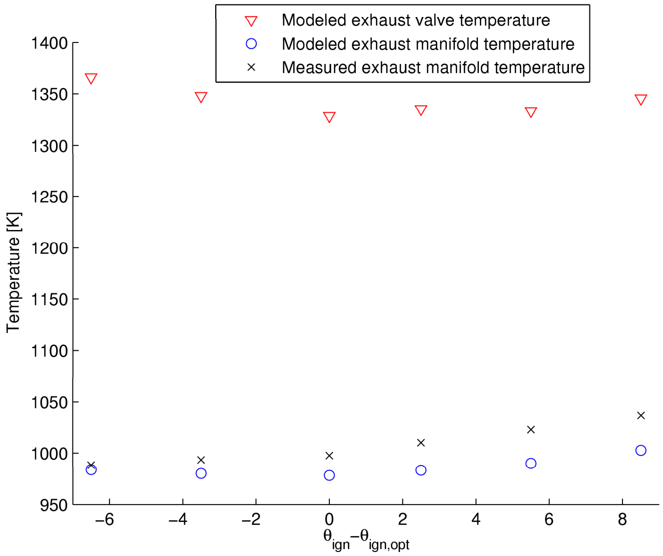

Figure 5.7. Modeled and measured temperatures when θ_{ign} is altered. There are signs that T_{ev} increases when θ_{ign} is moved from $\theta_{ign,opt}$. If that is the case, it is due to the reduced engine efficiency which leads to a higher exhaust temperature. It seems that the model has problems to capture variations in θ_{ign}, this may be due to the fact that γ_c and γ_e are estimated from the measurement points when $\theta_{ign} = \theta_{ign,opt}$.

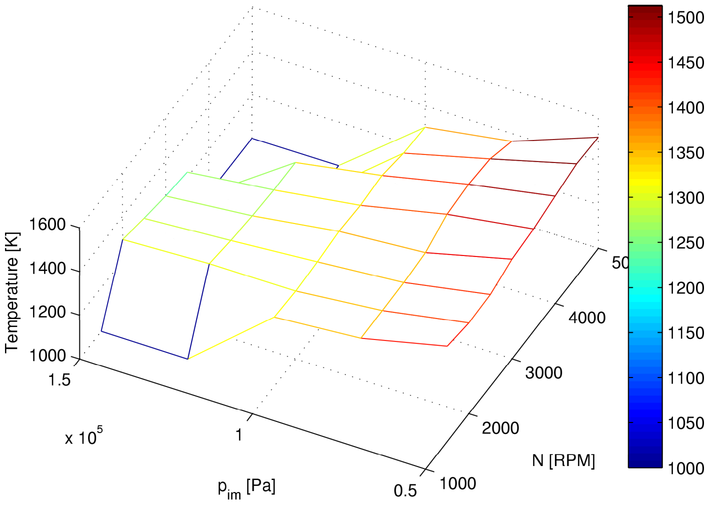

Figure 5.8. T_{ev} plotted against N and p_{im}. It can be seen that T_{ev} decreases with increasing p_{im}. T_{ev} is increasing with N at low loads but not on high loads. The reason T_{ev} is not increasing with N on high loads, may be that λ is not constant at these operating points. The engine operating points where fuel enrichment is made can be seen in figure 2.2 together with table 2.1. All blue lines represents measurement points that do not exist, but are created, in order to plot the mesh.

Chapter 6

Conclusion

The exhaust port temperature has been studied and a model has been built. Parameters such as manifold pressure, engine speed, ignition timing and air-to-fuel ratio have been changed and their influence on the exhaust port temperature has been investigated. The modeled mean temperature at the exhaust valve T_{ev}, depends mostly on these four variables:

- Intake manifold pressure p_{im}
- Engine speed N
- Air-to-fuel equivalence ratio λ
- Ignition timing θ_{ign}

The reader should have in mind that all the conclusions are based upon the model's behavior, since the temperature at the exhaust valve was not possible to measure. The discussion below shows effects that are visible in the model and data, but the explanations that are given are in most parts hypothesis that have not been verified or falsified.

6.1 T_{ev} decreases with increasing p_{im}

When p_{im} increases, T_{ev} decreases. A reasonable explanation may be that on high loads the difference between p_{EVO} and p_{em} is higher, which leads to a bigger expansion during the blowdown phase and a cooler gas temperature.

6.2 T_{ev} increases with N

T_{ev} increases with increasing N. An explanation is the shorter opening time of the intake and exhaust valves. This means that the gas cools down less around the valves. At higher speeds there is also more power that is transferred in the engine, which can result in a higher wall temperature and thus a higher gas temperature.

6.3 T_{ev}'s dependency of λ

Fuel enrichment affects the temperature in the cylinder in several ways. First by lowering the temperature at IVC due to the larger amount of fuel that is evaporating. Further on, the fuel enrichment also leads to incomplete combustion due to the lack of air for complete oxidation, which reduces the outgoing temperature after the combustion and expansion phase. There is also more mass to heat which reduces the temperature. When the air-fuel mixture is too lean T_{ev} also decreases. This is due to that the engine is more effective and a larger part of the fuels energy goes to the work production.

6.4 The ignition timings influence on T_{ev}

Moving the ignition timing from its optimal leads to increased T_{ev} due to decreased engine efficiency. Since θ_{ign} is just altered in the region ($\theta_{ign,opt}-6.5$, $\theta_{ign,opt}+8.5$) this is hard to see. It would be interesting to vary θ_{ign} in a bigger interval to see how it affects T_{ev}.

6.5 Correlation between mass flow and T_{ev}

No correlation between $\dot{m}$ and T_{ev} is seen, which is a contradiction to previous research [2], where the temperature is found to increase with increasing mass flow. However it should be noted that the model does not have an explicit mass flow dependence.

6.6 Future work

A logical continuation of the work would be to validate the model with new measurement data, to further validate and explore how good the model really is. It would also be of interest to extend the measurements of λ and θ_{ign} over more engine operating points. By studying the effects of altering λ and θ_{ign}, their influence on the exhaust temperature at different engine loads and engine speed can be evaluated. These conclusions can then be used in the analysis of the high load operating points, where fuel enrichment is used. With more advanced measurement equipment the estimation of h_{cv} can be enhanced. This means that the model of exhaust temperature can be verified. Another interesting approach would be to estimate T_{ev} through the energy equation from [6]:

$$m_e T_{ev} = \dot{m}_{af} c_p T_{im} + \dot{m}_f c_p T_f + \dot{m}_f q_{LHV} \eta_\lambda - \dot{m}_f q_{LHV} \widetilde{\eta}_{ig} - \dot{Q}_{ht} \tag{6.1}$$

An attempt was made to model T_{ev} this way, but failed since the heat transfer $\dot{Q}_{ht}$ is hard to estimate. A better known heat transfer would improve the results.

Nomenclature

The nomenclature used in the master thesis is defined below with variables, description of the variables and finally their respective units.

Var	Description	Unit
(A/F)	Air-to-fuel ratio	-
$(A/F)_s$	Stoichiometric air-to-fuel ratio	-
c_p	Specific heat at constant pressure	J/kgK
c_v	Specific heat at constant volume	J/kgK
h	Heat transfer coefficient	W/m^2
γ_c	Polytropic coefficient for the compression pressure	-
γ_e	Polytropic coefficient for the expansion pressure	-
M	Torque	Nm
m_t	Total mass in the cylinder	kg
m_a	Mass of air in the cylinder	kg
m_f	Mass of fuel in the cylinder	kg
m_{af}	Mass of air and fuel in the cylinder	kg
m_r	Mass of residual gases in the cylinder	kg
$\dot{m}$	Mass flow	kg/s
$\dot{m}_{at}$	Mass flow air at throttle	kg/s
N	Engine speed	rpm
n_r	Number of engine revolutions per cycle	-
p_{cyl}	Measured cylinder pressure	Pa
p	Modeled cylinder pressure	Pa
p_{im}	Intake manifold pressure	Pa
p_{em}	Exhaust manifold pressure	Pa
p_c	Compression pressure asymptote	Pa
p_e	Expansion pressure asymptote	Pa
q_{HV}	Heating value	J/kgK
R	Mass specific gas constant	J/kgK
r_c	Compression ratio	-
$t_{inj_{1-4}}$	Fuel injection time cylinder 1-4	s
T_{im}	Temperature at intake manifold	K

Var	Description	Unit
T_w	Mean value temperature of wall sensors in the exhaust manifold	K
T_{eb}	Temperature at engine block	K
T_{ev}	Modeled mean value temperature at the exhaust valve	K
T_{em}	Modeled temperature at the exhaust manifold	K
$T_{em,meas}$	Measured temperature at the exhaust manifold	K
U,u	Internal energy U=mu	J, J/kg
V,v	Volume and specific volume	m^3, m^3/kg
V_c	Clearance Volume	m^3
V_d	Displaced Volume	m^3
V_{tot}	Total cylinder volume	m^3
W	Work	J, Nm
Q	Heat	J
$\dot{Q}_{ht}$	Heat transfer rate	W = J/s
$\dot{q}$	Heat flux, heat transfer per unit time and unit area	W/m^2
λ	Air-to-fuel equivalence ratio (normalized (A/F))	-
η_{vol}	Volumetric efficiency	-
θ	Crank Angle	degree

Abbreviation

Abbreviations that are used are defined below:

Abbreviation	Meaning
BDC	Bottom dead center
BL	End of blowdown phase
BMEP	Brake mean effective pressure
BTDC	Before top dead center
EVO	Exhaust valve opening
EVC	Exhaust valve closening
IMEP	Indicated mean effective pressure
IVO	Inlet valve opening
IVC	Inlet valve closening
MBT	Maximum Brake Torque
MEP	Mean effective pressure
MFB	Mass fraction burned
MVM	Mean value model
TDC	Top dead center

Subscripts

Subscripts that are used are defined below:

Subscript	Description
a	Ambient
af	Air and fuel
cd	Conduction
cv_i	Convection internal
cv_i	Convection external
e	Engine
g	Gas
i	Intake system, inlet or internal
o	Outlet or outer
rad	Radiation
w	Wall

Bibliography

[1] Per Öberg and Lars Eriksson. *Control Oriented Gas Exchanged Models for CVCP Engines and their Transient Sensitivity*. Institut francais du pétrole, 2007.

[2] Lars Eriksson. *Mean Value Models for Exhaust System Temperatures*. Society of Automotive Engineers Inc., 2002.

[3] J. B. Heywood. *Internal Combustion Engine Fundamentals. McGraw-Hill series in mechanical engineering*. McGraw-Hill, 1988.

[4] Kenneth Kar, Stephen Roberts, Richard Stone, Martin Oldfield, and Boud French. *Instantaneous Exhaust Temperature Measurements Using Thermocouple Compensation Techniques*. Society of Automotive Engineers Inc., 2003.

[5] Ingemar Andersson Lars Eriksson. *An Analytic Model for Cylinder Pressure in a Four Stroke SI Engine*. Society of Automotive Engineers Inc., 2002.

[6] Lars Nielsen Lars Eriksson. *Modeling and Control of Engines and Drivelines*. Vehicular systems, ISY, Linköping Institute of Technology, 2 edition, 2008.

[7] Michael Mladek and Christopher H.Onder. *A Model for the Estimation of Inducted Air Mass and the Residual Gas Fraction using Cylinder Pressure Measurements*. Society of Automotive Engineers Inc., 2000.

[8] Anthony Sorin, Francois Bouloc, Brahim Bourouga, and Pierre Anthoine. *Experimental study of periodic heat transfer coefficient in the entrance zone of an exhaust pipe*. Elsevier Masson SAS, 2008.

[9] Andreas Wimmer, Robert Pivec, and Theodor Sams. *Heat transfer to the combustion chamber and port walls of ic-engines - measurements and predictment. In SP-1511, Modeling of SI-engines , number 2000-01-0568 in SAE Technical Papers, pages 101-116, March 2000*. Oldenbourg Verlag, 2003.